Polymer Degradation and Stability 187 (2021) 109544

Contents lists available at ScienceDirect

Polymer Degradation and Stability

journal homepage: www.elsevier.com/locate/polymdegradstab

High-efficiency phosphorus/nitrogen-containing flame retardant on epoxy resin

Donghui Wang[a], Quanyi Liu[a,*], Xiaoliang Peng[a], Chuanbang Liu[a], Zekun Li[a], Zhifa Li[a], Rui Wang[a], Penglun Zheng[a,*], Hui Zhang[b,*]

[a] College of Civil Aviation Safety Engineering, Civil Aviation Flight University of China, Guanghan, 618307, China
[b] Institute of Public Safety Research, Tsinghua University, Beijing 100084, China

ARTICLE INFO

Article history:
Received 25 November 2020
Revised 22 February 2021
Accepted 28 February 2021
Available online 3 March 2021

Keywords:
Epoxy resin
Flame retardancy
Lower phosphorus content
Gas phase
Condensed phase

ABSTRACT

A phosphorus/nitrogen-containing compound (named DOPO-BAPh) was synthesized via the graft reaction between 9,10-dihydro-9-oxa-10-phosphaphenanthrene-10-oxide (DOPO) and bisphenol A bis(phthalonitrile) containing benzoxazine. The flame retardancy of DOPO-BAPh was investigated on epoxy resin (EP). The results showed that DOPO-BAPh catalyzed the curing reaction of due to the phenolic hydroxyl groups in the structure. The nitrile group in DOPO-BAPh was self-cured in EP to form cross-linked networks containing aromatic heterocycles, further enhancing the stability of the char layer formed after combustion. The introduction of DOPO-BAPh strengthened flame retardancy of the EP. With only 0.26 wt.% phosphorus of loading level, the modified EP reached an LOI value of 35.8% and obtained V-0 rating in UL-94 testing. And DOPO-BAPh exhibited char-forming ability during the decomposition. Besides, the DOPO-BAPh showed flame-retardant activity in both the gas and condensed phases.

1. Introduction

Epoxy resin (EP), as a promising thermosetting polymer, has been widely applied in a variety of applications as laminating, adhesive, coating, and casting fields owing to the satisfactory electrical insulation, superior adhesion property, and chemical resistance. However, the defects of high fire hazard have restricted its application in high-performance areas, such as in the aviation industry [1-3]. It is urgent to impart flame resistance to EPs. Recently, many efforts have been made by numerous researchers to achieve the flame retardation of EP. One of the most widely used approaches is the use of flame-retardant additives [4,5]. Halogen-containing compounds are considered to be one of the most effective ways to enhance the flame retardancy of polymers. However, the gaseous toxic products produced during the combustion of compounds containing halogens cause irreversible damage to human health and environmental safety. Currently, halogen-free flame retardants have received extensive interest from researchers [6-8].

At present, the halogen-free flame-retardant systems used in EPs include phosphorus-containing compounds [9-11], nitrogen-containing compounds [12,13], silicon-containing compounds [14,15], metal oxides [16] and nano-fillers [17,18]. Especially, phosphorus-containing compounds have been regarded as an efficient flame retardant due to their high-efficiency flame retardancy. The significant merits of replacing halogens with phosphorus include high flame-retardant efficiency, less toxic products produced in flames, and less damage to the environment. Among phosphorous compounds, 9,10-dihydro-9-oxa-10-phosphaphenanthrene-10-oxide (DOPO) and its derivatives are widely applied to provide flame retardancy to EPs owing to their fire resistance and eco-friendly [19]. The structure of DOPO contains the P-H bond, which can generate numerous derivatives through nucleophilic addition reactions with various functional groups. DOPO and its derivatives exhibit thermal and chemical stability due to their molecular structure containing biphenyl and phenanthrocyclic structures, especially the side phosphorus groups introduced by the cyclic O=P-O bonding mode. However, the limitation of phosphorus content in phosphorus-containing EPs leads to low flame-retardant efficiency. It has been reported that flame-retardant efficiency can be significantly improved by introducing flame retardant groups into DOPO-based derivatives, such as phosphate [20], nitrogenous [21], silicious [22] and borate [23], etc. Wang, et al., constructed a nitrogen/sulfur-containing DOPO-based compound (SFG). The resulting EP/SFG composites with 0.38 wt.% phosphorus content obtained UL-94 V-0 rating and an LOI value of 32.8% [24]. Zhu,

* Corresponding author
E-mail addresses: quanyiliu2005@cafuc.edu.cn (Q. Liu), zhengpenglun@cafuc.edu.cn (P. Zheng), zhhui@tsinghua.edu.cn (H. Zhang).

https://doi.org/10.1016/j.polymdegradstab.2021.109544
0141-3910/

et al., reported a phosphorus-nitrogen flame retardant (MAPPO) for EPs. The flame-retardant EP with 18 wt.% MAPPO reached UL-94 V-0 rating and with an LOI value of 33% [25]. Luo, et al., designed a phosphorus–nitrogen–silicon compound (DPHK) with simultaneously improved flame-retardant properties and smoke suppression. The resulting modified EP containing 3% DPHK scored UL-94 V-0 rating and obtained an LOI value of 29% [26]. Tang, et al., synthesized a compound (ODOPB-borate) containing DOPO and borate to strengthen the flame retardancy of EP. The test results showed that ODOPB-borate imparted flame retardancy to EP through charring ability and flame inhibition effect [27]. Therefore, the combination of multiple elements has become one of the most popular approaches for imparting flame retardancy to EPs.

Nitrogen compounds can be used alone as flame retardants or as additives to other flame-retardant elements (e.g. phosphorus) to increase their activity. Phthalonitrile, a nitrogen-containing compound, has attracted wide attention from researchers due to outstanding thermal properties, mechanical properties and flame retardancy [28]. The nitrile groups of phthalonitrile can form a complex aromatic heterocyclic with cross-linking networks through polymerization [29]. The introduction of this cross-linked network structure into the polymers not only improves the flame retardancy and thermal stability but also effectively prevents the migration of additives from the interior of the polymer to the surface. Consequently, according to previous studies, the design of DOPO derivative structures with nitrogen-containing compounds is regarded as an efficient approach to enhance flame-retardant efficiency [30,31].

In this study, a DOPO-based compound (DOPO-BAPh) by using DOPO and bisphenol A bis(phthalonitrile) containing benzoxazine (BAPh) was added to EPs as an additive to evaluate the effect to the flame-retardant efficiency of EPs. The chemical structure, curing behaviours, thermal stability, flame retardancy, and flame-retardant mechanism of modified EPs are investigated. DOPO-BAPh with phenolic hydroxyl group promotes the curing reaction of EPs. The introduction of DOPO-BAPh imparts enhanced flame-retardant properties to EPs, and DOPO-BAPh works at both the gas phase and condensed phase.

2. Materials and methods

2.1. Materials

Diglycidyl ether of biphenol A (DGEBA, E-51, epoxide value of 0.51 mol/100 g) was produced from Shandong Jiaying Chemical Technology Co., Ltd., China. The 4, 4'-diaminodiphenylsulphone (DDS) was purchased from Wenzhou Shoucheng Chemical Technology Co., Ltd. DOPO was purchased from Adamas-beta®. The phthalonitrile-based resin containing benzoxazine was purchased from Chengdu Dymatic Fine Chemicals Co., Ltd.

2.2. Synthesis of DOPO-BAPh

BAPh (73.8g, 0.1 mol) and DOPO (43.2g, 0.2 mol) were added to a triple flask containing 400 ml of tetrahydrofuran (THF). The reaction was protected by nitrogen throughout the entire process. The mixture was stirred at 80°C and refluxed for 12 hours. At the end of the reaction, the residual solvent was eliminated by using a rotary evaporator. Finally, the targeted product DOPO-BAPh was obtained by washing in ethanol and drying at 60°C for 12 hours. The synthetic route of DOPO-BAPh is shown in **Scheme 1**. FTIR(KBr, cm^{-1}):2231 (-CN),3408 (-OH), 1430 (P-Ph),1248 (P=O),913 (P-O-Ph). ^{1}H-NMR (DMSO-d_6, ppm):9.2-9.3(-OH, 2H), 6.5-8.3(Ar-H, 36H), 4.0-4.4(-CH_3, 6H), 1.0-1.5(-CH_2-N_2-CH_2-, 8H). ^{31}P-NMR (DMSO-d_6, ppm):31.4 and 32.2.

2.3. Preparation of flame-retardant EP composites

The epoxy thermosets were obtained using thermally curing. First, the EP is heated at 100°C for about 10 minutes to flow state. The DDS powder was homogeneously dispersed by mechanical stirring at 100°C to obtain a transparent mixture. Then, stir continuously until the mixture is clear and transparent, and add DOPO-BAPh and continue stirring for 10 min to make DOPO-BAPh dispersed in the mixture. Finally, the mixture was dumped onto the curing mold coated with the release agent. and the curing reaction was initiated according to different heat treatment temperatures. The heat treatment temperatures for the curing reaction are 190°C, 4h; 210°C, 2h; 230°C, 2h; 250°C, 2h; and 270°C, 2h. The contents of EP, DOPO-BAPh, and DDS are presented in **Table 1**.

2.4. Characterization

The Fourier-transform infrared (FTIR) spectra were tested on a Spectrum Two spectrometer (Perkin-Elmer, USA) using the KBr pellets method in the frequency range of 4000 to 450 cm^{-1}.

^{1}H-NMR and ^{31}P-NMR spectra were both got from a Bruker Avance III-400 NMR spectrometer (400 MHz), and the DMSO-d_6 was served as the solvent.

The differential scanning calorimetry (DSC) spectra were received through heating the sample (around 5mg) from room tem-

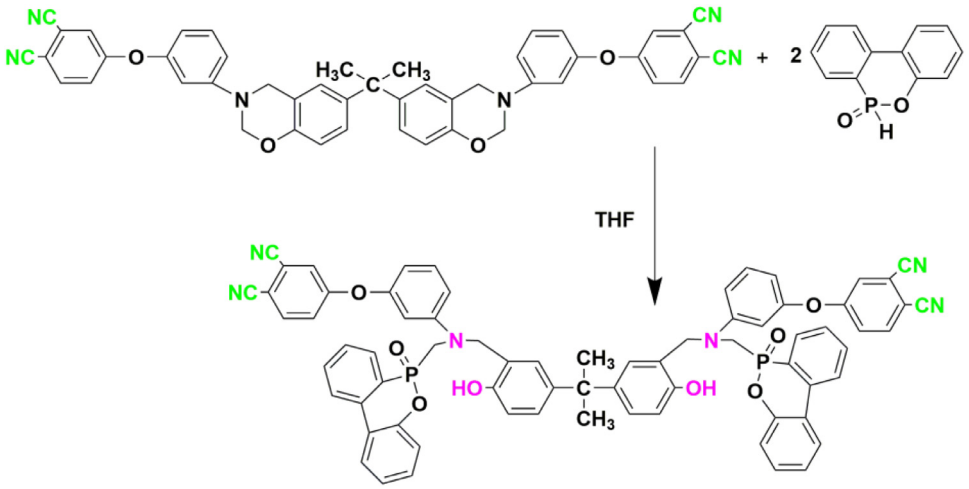

Scheme 1. Synthetic route of DOPO-BAPh

Table 1
Formulas of epoxy thermosets.

Samples	Composition(phr)	Content of DOPO-BAPh (wt.%)		Content of P (wt.%)
		Cured EPs	DOPO-BAPh	
EP	100	0	0	0
5DOPO-BAPh/EP	100	5	3.79	0.26
10DOPO-BAPh/EP	100	10	7.29	0.50
15DOPO-BAPh/EP	100	15	10.6	0.71
20DOPO-BAPh/EP	100	20	13.6	0.91

perature to 300°C at 5°C/min with a DSC 4000 instrument (Perkin-Elmer, USA), and the nitrogen was blown in throughout the process. The flow rate of nitrogen was 20ml/min.

The value of limiting oxygen index (LOI) was obtained from the JF-3 oxygen index meter (Nanjing Jiangning Instrument Factory, China). The procedure and the dimensions (100 × 6.5 × 3 mm^3) were all base on the GB/T2406-93. Ten identical samples were used for each set of tests.

The UL-94 ratings were rated by the testing procedure of ASTM D 3801 on a CZF-3 instrument (Nanjing Jiangning Instrument Factory, China) with a sample size of 100 × 13 × 3 mm^3. The burning grade of the sample was classified as V-0, V-1, V-2 or NR (unclassified), according to its burning behaviour.

The cone calorimeter test was measured by a cone calorimeter 6810 (Shuzhou Yangyi Vouch Testing Technology, China) instrument. The sample size (100 × 100 × 3 mm^3) and heat flux (50kW/m^2) complied with ISO 5660-1 protocol. The test on each sample was repeated three times and the error repeatability of the data was within ±5%.

Dynamic mechanical analysis (DMA) was measured with a DMA 850 (TA instrument, USA) in the three-point bending mode with an amplitude of 15 μm and a frequency of 1 HZ. The test temperature ranged from 30~300°C at a rate of 10°C/min. The dimensions of the samples were 50 mm × 8 mm × 4mm. The test on each sample was repeated three times.

Thermogravimetric analyses (TG) were obtained after heating the samples (around 10 mg) from room temperature to 800°C at 10°C /min with Pyris thermogravimetric analyser (Perkin-Elmer TGA 4000, USA), and the nitrogen was blown in throughout the process.

The thermogravimetry–infrared spectroscopy (TG-IR) was performed on a system that was build up by a TGA 4000 thermogravimetric analyser and a Spectrum Two FTIR spectrophotometer. The process of TG-IR was similar to that of TG which means the sample will go through the same heat treatment procedure (30°C-800°C, 10°C/min) under the gas flow of nitrogen.

The microscopic morphologies of residual chars that were conducted by a Hitachi S-4800 scanning electron microscope (SEM) with an accelerating voltage of 5 kV. The measurement was performed using residual char after cone calorimeter test. The surface of samples was coated with a layer of gold prior to testing.

X-ray photoelectron spectroscopy (XPS) was determined on a Thermo Scientific K-Alpha+ spectrometer with Mono AlKa excitation source. The layer on top of the residual chars after the cone test was chosen as the sample for testing.

3. Results and discussion

3.1. Structural characterizations of DOPO-BAPh

The structure of DOPO-BAPh was determined by FTIR, ^{1}H-NMR, and ^{31}P-NMR spectroscopy. Fig. 1 presents the FTIR spectra of DOPO, BAPh, and DOPO-BAPh. The characteristic peak at 2436 cm^{-1}, 1428 cm^{-1}, 1239 cm^{-1}, and 904 cm^{-1} are assigned to the P-H bonds, P-Ph, P=O, and P-O-Ph stretching vibrations of DOPO

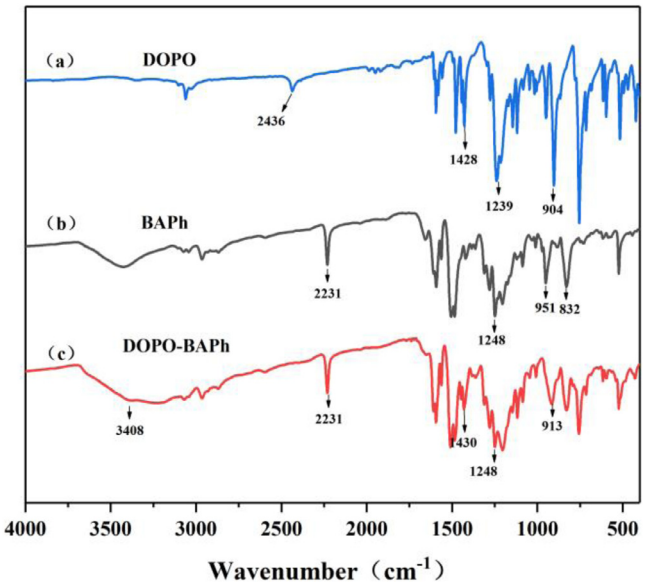

Fig. 1. FTIR spectrum of DOPO, BAPh and DOPO-BAPh.

[32]. In the spectrum of BAPh, the characteristic absorption peak of -CN is detected at 2231 cm^{-1} and the same spikes are detected in the spectrum of DOPO-BAPh [33]. The peak at 951 cm^{-1} is corresponding to the characteristic absorption peak of the oxazine ring [34]. Besides, the characteristic absorption peaks of the C-O-C and C-N-C telescopic vibrations occur at 1248 cm^{-1} and 832 cm^{-1}, respectively [34]. In the spectrum of DOPO-BAPh, it is noticed that the -OH characteristic peak at 3408 cm^{-1} widened significantly while the P-H (2436cm^{-1}) bond and oxazine ring (951cm^{-1}) disappeared [32]; The characteristic peaks of P-O-Ph and P-Ph stretching absorption appeared at 913 cm^{-1} and 1430 cm^{-1}, and the characteristic peaks P=O stretching absorption at 1248 cm^{-1} overlaps with the C-O-C stretching. The results indicate that DOPO-BAPh was prepared successfully.

The ^{1}H NMR spectra of DOPO-BAPh is presented in Fig. 2(a). DOPO-BAPh exhibit the chemical shifts of Ar-H at 6.45-8.35 ppm. Signals corresponding to -OH protons are observed at 9.29 and 9.35 ppm. The proton peak of -CH_3 in bisphenol A appears at 4.01-4.49 ppm, -N-CH_2- at 0.93-1.69 ppm. The ratio of the integral areas of Ar-H, -OH, -CH_3 and -N-CH_2- in the spectra is 36:1.93:6.34:8.07, which is consistent with the ratio of the corresponding hydrogen atoms in DOPO-BAPh. As shown in Fig. 2(b), signals of 31.4 and 32.2 ppm are noted in the ^{31}P-NMR spectrum of DOPO-BAPh. It is hypothesized that steric hindrance effects between the small amount of by-products (Phthalocyanine ring and triazine ring) in DOPO-BAPh and DOPO groups lead to the formation of stereoisomers with unequal phosphorus peaks [5,35]. The small peak near 15 ppm is attributed to a few unreacted DOPO.

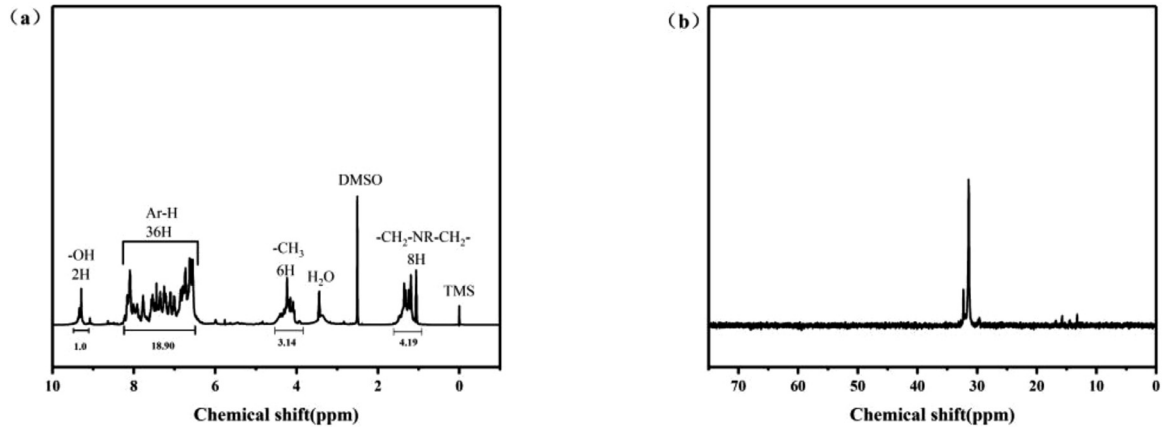

Fig. 2. (a) ^{1}H-NMR and (b)^{31}P-NMR spectrum of DOPO-BAPh.

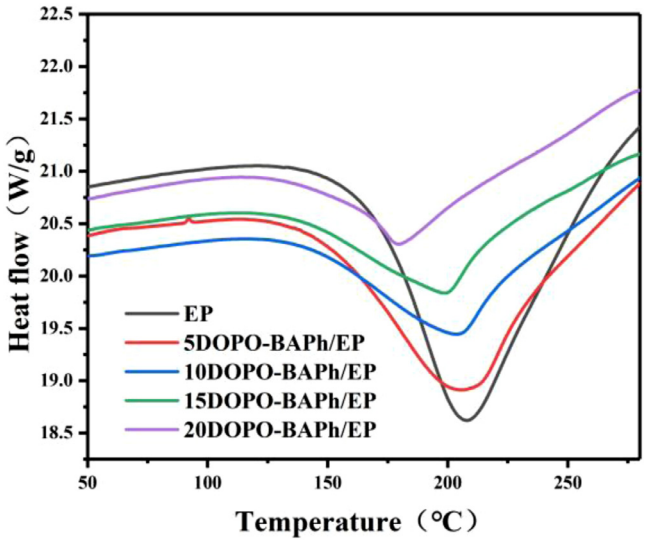

Fig. 3. Curing behaviours of DDS and DOPO-BAPh/EP blends.

3.2. Curing behaviors

The curing behaviours of DOPO-BAPh/EP with DDS blends were investigated by DSC at a heating rate of 5°C/min. The results are illustrated in Fig. 3. As shown in the figure, all samples show a single exothermic peak, which is relative to the curing reactions of the EP. Furthermore, the curing peak shift to a low-temperature range with the increasing DOPO-BAPh content. The curing exothermic peak of 20% DOPO-BAPh/EP occur at 179°C, which was 29°C lower than EP. The results suggest that DOPO-BAPh facilitated the curing reaction of EP. The structure of DOPO-BAPh contains Mannich bridge (-CH_2-NR-CH_2) with hydroxyl groups, and the epoxy groups can be opened up by hydroxyl group, thus promoting the curing reaction of EP [34,36]. As the content of DOPO-BAPh increase, more hydroxyl groups are added to the EP, catalysing the curing reaction.

3.3. Flame retardancy of EP composites

The results of LOI value and UL-94 tests are shown in Table 2. The LOI value of EP is only 21.7%, and fail to pass the UL-94 test. With the 5wt.% addition of DOPO-BAPh, the LOI of epoxy thermoset increase to 35.8%. The LOI value of epoxy thermoset can be further improved by increasing the addition of DOPO-BAPh. As the content of DOPO-BAPh increase to 20 wt.%, the LOI grew to 41.2%.

Table 2
LOI value and UL-94 rating of epoxy thermosets.

Samples		UL-94		
	LOI (%)	t_1+t_2(s)	Dripping	Rating
EP	21.7±0.2	>100s	Yes	NR
5DOPO-BAPh/EP	35.8 ±0.2	1.5s+4.5s ±0.5	No	V-0
10DOPO-BAPh/EP	39.7 ±0.2	1.3s+3.5s ±0.5	No	V-0
15DOPO-BAPh/EP	40.5 ±0.3	1.2s+1.5s ±0.5	No	V-0
20DOPO-BAPh/EP	41.2 ±0.3	1.0s+1.2s ±0.5	No	V-0

And all the modified epoxy thermosets pass the UL-94 V-0 test. In addition, the ratio between DOPO-BAPh and EP affect the flame retardancy of the samples. It is observed that the growth rate of LOI decelerate obviously when the incorporation of DOPO-BAPh exceed 10 wt.%, which is attributed to the addition of DOPO-BAPh resulting in a deviation from the optimal ratio between DOPO-BAPh and EP.

The burning of the epoxy thermosets during the UL-94 test was obtained with a digital camera. Fig. 4 shows some snapshots of epoxy thermosets. The EP burned rapidly after flame application and remain burning for more than 100 s with melt dripping. And all the modified epoxy thermosets were self-extinguishing without drippings within 10 seconds after extinguishing the flame thus scoring V-0 rating in UL-94 test. In addition, during the application of the flame to the modified epoxy thermosets, gas ejection from the surface of the sample was observed. The blowing-out effect refers to the concentrated ejection of pyrolysis gases from the interior of the char layer, which inhibits the continuous burning of the flame. The same phenomenon was observed by Yang [37] et al. who named the "blowing-out extinguishing effect". The results indicate that the DOPO-BAPh exhibit effectiveness in enhancing the flame-retarding effect of epoxy thermosets.

The combustion of epoxy thermosets with various additive loads was tested via cone calorimeter testing. Fig. 5 shows the heat release rate (HRR) curves. The combustion parameters are shown in Table 3, including the time to ignition (TTI), peak HRR (PHRR), total heat release (THR), average-effective heat of comb (av-EHC), total mass loss rate (TML) and total smoke release (TSR). It was found that TTI decreased significantly with increasing DOPO-BAPh addition. The earlier decomposition of DOPO-BAPh triggers the pyrolysis of the epoxy matrix, which facilitate the formation of char during the combustion and impart flame retardancy to epoxy thermosets.

It can be seen from Fig. 5, the EP burns rapidly after ignition, reach a sharp peak with a PHRR of 1064.0 kW/m^2 and a THR of 97.1 MJ/m^2. The presence of DOPO-BAPh in epoxy ther-

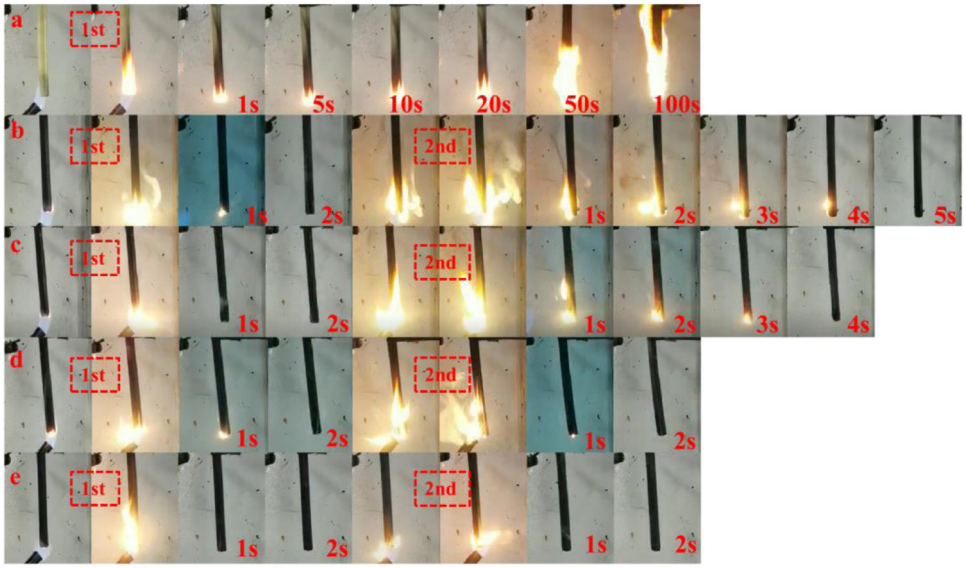

Fig. 4. Video snapshots of epoxy thermosets during the UL-94 test. (a: EP; b: 5DOPO-BAPh/EP; c: 10DOPO-BAPh/EP; d: 15DOPO-BAPh/EP; e: 20DOPO-BAPh/EP, 1st means the first application of flame;2nd means the second application of flame).

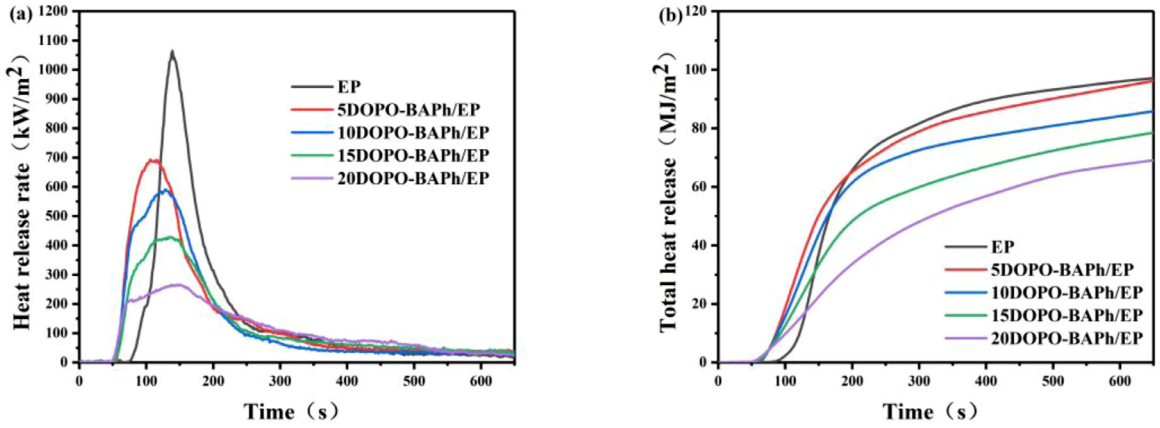

Fig. 5. (a) Heat release rate and (b) total heat release rate curves of epoxy thermosets at a heat flux of 50 kW/m^2.

Table 3
Burning parameters of epoxy thermosets obtained from cone calorimeter tests.

Samples	TTI(s)	PHRR(kW/m^2)	THR(MJ/m^2)	av-EHC(MJ/kg)	TSR(m^2/m^2)	TML(%)
EP	59 ±2	1064 ±60	97.1 ±10	35.9 ±1.9	2952 ±98	96.8 ±3
5DOPO-BAPh/EP	54 ±1	693 ±23	96.2 ±11	33.4 ±1.6	2747 ±93	88.6 ±5
10DOPO-BAPh/EP	53 ±1	591 ±24	85.9 ±8	31.3 ±1.3	2583 ±85	85.3 ±4
15DOPO-BAPh/EP	51 ±2	429±22	78.6 ±8	28.7 ±1.3	2541 ±75	82.8 ±5
20DOPO-BAPh/EP	47 ±2	266±13	69.1 ±9	26.3 ±1.1	2481 ±72	77.7 ±4

mosets result in a marked reduction in PHRR. Typically, the PHRR of 20DOPO-BAPh/EP decreased to 266.0 kW/m^2, the value of which is reduced by 75.6% in comparison to EP. Compared with the EP, The THR of 20DOPO-BAPh/EP thermoset decreased by 28.8%. The reduced values of THR and HRR indicate that the introduction of DOPO-BAPh imparts flame retardancy to epoxy thermosets.

The flame retardant properties of DOPO-BAPh/EP composites are further investigated by av-EHC, TSR and TML. It is observed from Table 3 that av-EHC, TSR and TML are also reduced with the incorporation of DOPO-BAPh. The EHC values reflect the degree of combustion of combustible gases in the gas phase. As shown in Table 3, The av-EHC of epoxy thermosets show a downward trend with the increasing content of DOPO-BAPh. The av-EHC of 5DOPO-BAPh/EP is 7% lower than EP, as the addition of DOPO-BAPh increased, the av-EHC was further reduced. The addition of DOPO-BAPh induced the decomposition of the epoxy thermosets to generate free radicals and non-flammable gases, which suppresses the flame activity of the gas phase, thus revealing the flame-retardant effect of DOPO-BAPh in the gas phase. In addition, it is noted from Table 3 that the value of TML decreases with increasing content of DOPO-BAPh. The lower TML value means that more char residues were generated. The generation of char residues plays a crucial role in limiting the transformation of fuel to gas. Therefore, the introduction of DOPO-BAPh promoted the generation of the chars in the combustion of epoxy thermosets, providing the flame-retarding effect in the condensed phase. Meanwhile the values of TSR are reduced with the incorporation of DOPO-BAPh. The reason is due to the gaseous fragments generated by the degradation of the epoxy

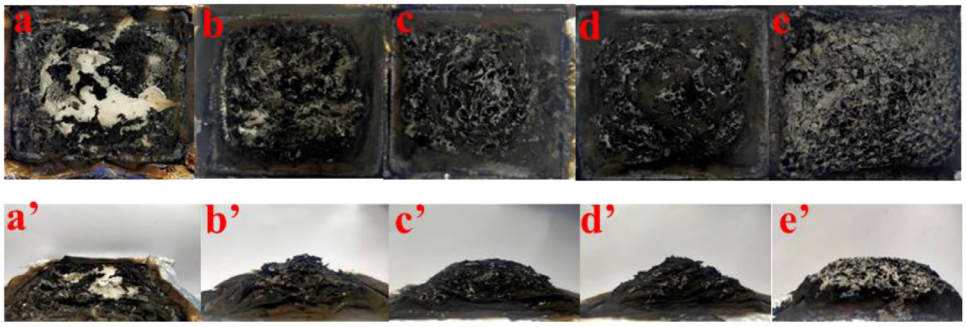

Fig. 6. Video screenshots of char residues from cone calorimeter tests of (a and a') EP, (b and b') 5DOPO-BAPh/EP, (c and c') 10DOPO-BAPh/EP, (d and d') 15DOPO-BAPh/EP, (e and e') 20DOPO-BAPh/EP.

matrix are retained in the residue, while DOPO-BAPh promotes the formation of more char residues.

The video screenshots of char residues from cone calorimeter tests are presented in Fig. 6. It is clear that the char layer of EP was extremely thin and the bottom foil was broken. In contrast that the introduction of DOPO-BAPh improved the integrity and stability of the char layer formed by the combustion of epoxy thermosets. The char layers of modified epoxy thermosets became denser and more expanded. The char layer can make a significant contribution in inhibiting the transmission of heat and oxygen and also reducing the exposure of the underlying epoxy matrix to thermal radiation, which suppressed the thermal decomposition of the epoxy thermosets [38,39]. The contribution of hydroxyl and phospho-phenanthroline groups is an important factor in the formation of char layers [39,40]. Another reason may be ascribed to the presence of nitrile groups in DOPO-BAPh, which can form the stable network-structure through self-cured [41,42]. Such a network structure reinforced the stability of the char layer formed by combustion. At the same time, the dense carbon layer has the ability to hold more of the non-combustible gases generated by combustion, resulting in the more expanded char layer. Therefore, the addition of DOPO-BAPh promoted the formation of the dense char layer, which reduced the effect of radiated heat on the underlying epoxy matrix.

3.4. Thermal analysis of EP composites

The T_g of epoxy thermosets was determined by DMA. The peak of Tan δ is the T_g of epoxy thermosets. Fig. 7 shows the curve of Tan δ of epoxy thermosets as a function of temperature. EP shows a T_g of 182.3°C. It is observed that T_g increased with the addition of a small amount of DOPO-BAPh. The T_g of 5DOPO-BAPh/EP thermoset is found to be 204°C. However, further increase of DOPO-BAPh content in epoxy thermosets resulted in a decrease of T_g. For example, the T_g of 15DOPO-BAPh/EP and 20DOPO-BAPh/EP are 171.7°C and 164.7°C, respectively. When the loading of DOPO-BAPh is low, a minor portion nitrile group in DOPO-BAPh reacts with the EP by copolymerization in the pre-curing stage, thus enhancing the crosslink density. Generally, the high crosslink density after curing implies high T_g. When the loading of DOPO-BAPh further increases, the higher loading of DOPO-BAPh result in a deviation from the optimal ratio. Excess addition of DOPO-BAPh forms phthalocyanines with large molecular chains after curing leading to a decrease in crosslink density.

The thermal stability of DOPO-BAPh/EP composites under the nitrogen atmosphere was investigated by thermogravimetric analysis. Fig. 8 shows the TG and derivative thermogravimetric (DTG) curves for epoxy thermosets in a nitrogen atmosphere. Summary of the TGA results of epoxy thermosets under N_2 atmosphere is presented in Table 4. The graph shows only one sharp weight-loss stage during the entire heating process, which is attributed to chain breaks in the polymer structure. This result demonstrates that the thermal degradation mechanism of EP is not altered by the introduction of DOPO-BAPh. And the degradation of the EP in nitrogen gas mainly occur from 379°C to 550°C with about 80% weight loss. The onset degradation temperature (T_{onset}), temperature at 5% weight loss ($T_{5\%}$) and the temperatures of maximum weight loss rate (T_{max}) decreased with the increasing content of DOPO-BAPh, indicating the reduced in the thermal stability of EP, which is attributed to the early initial decomposition of DOPO-BAPh. In addition, the char yield at 700°C of 20DOPO-BAPh/EP achieve 31.5%, approximately 100% improvement to EP. The higher char yield is attributed to the facilitation of char formation by DOPO-BAPh. Generally, the early degradation of DOPO-BAPh under combustion facilitated the generation of chars in the condensed phase, as evidenced by the high char yield, which was identical to the flame-retardant mechanism of the condensed phase obtained

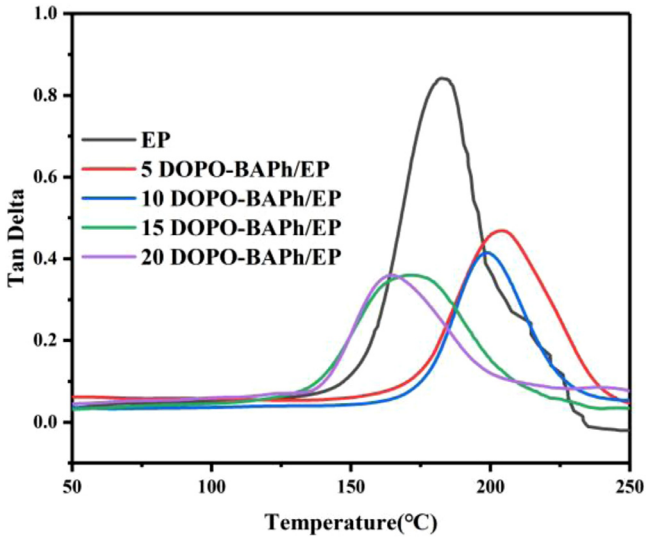

Fig. 7. DMA curves of epoxy thermosets.

Table 4
Summary of the TGA results of epoxy thermosets under N_2 atmosphere.

Samples	T_{onset} (°C) ±2	$T_{5\%}$(°C) ±2	T_{max}(°C) ±2	C_{y700}(%) ±1
DOPO-BAPh	277.2	290.1	413.9	68.0
EP	379.5	397.3	428.5	15.6
5DOPO-BAPh/EP	373.8	380.7	417.0	23.5
10DOPO-BAPh/EP	368.3	380.0	404.3	26.8
15DOPO-BAPh/EP	356.6	364.6	398.4	28.5
20DOPO-BAPh/EP	341.4	349.4	384.8	31.5

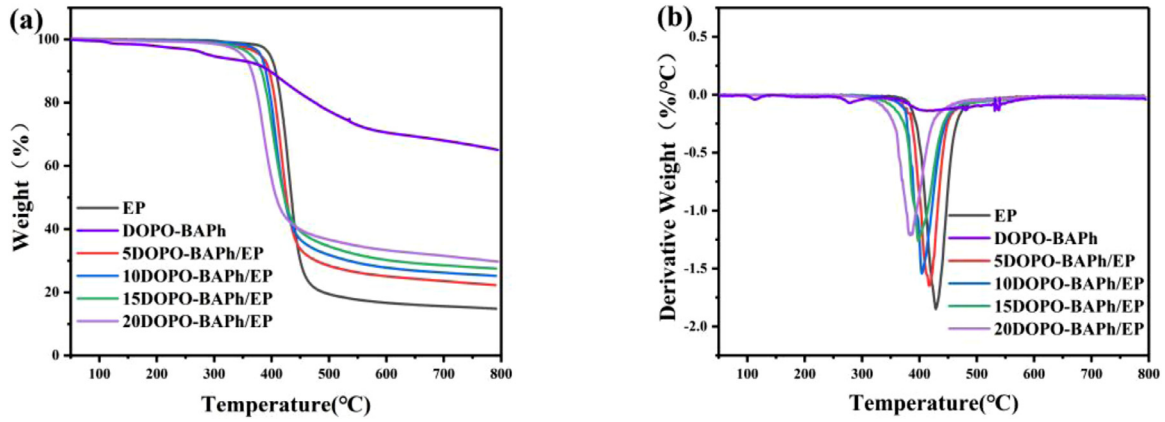

Fig. 8. (a)TGA and (b)DTG curves of DOPO-BAPh and epoxy thermosets under N_2 atmosphere.

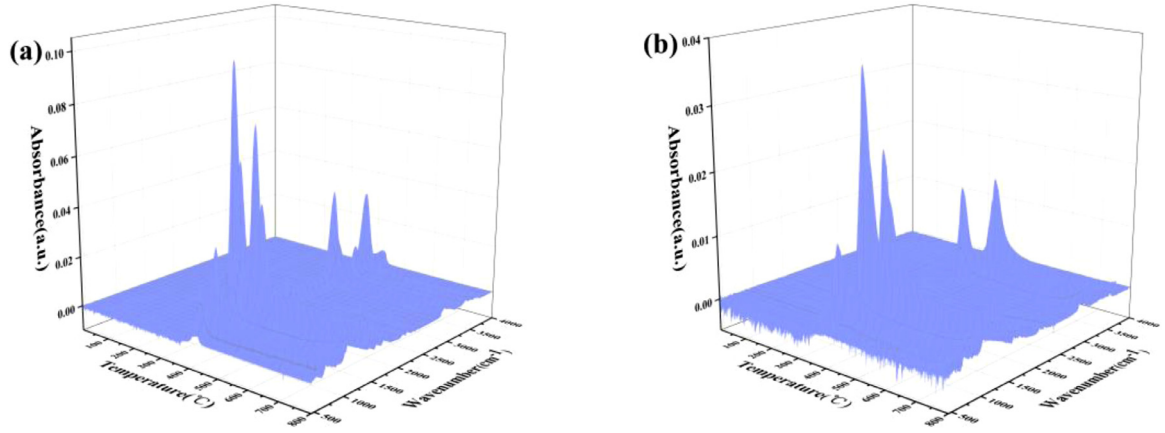

Fig. 9. TG-IR 3D images of (a) EP and (b) 20DOPO-BAPh/EP.

in cone tests. Meanwhile, the nitrile group improves the stability of the char, further retards the decomposition of the char.

3.5. TG-IR analysis of EP composites

To explore the flame-retardant effect of DOPO-BAPh on EP in the gas phase, the pyrolysis products of epoxy thermosets during pyrolysis under the nitrogen atmosphere was characterized using TG-IR. Fig. 9(a) and Fig. 9(b) show the 3D images of the pyrolysis products during the decomposition of EP and 20DOPO-BAPh/EP composite. The characteristic spectra of the pyrolysis products of EP and 20DOPO-BAPh composite at different stages of decomposition are shown in Fig. 10(a) and Fig. 10(b). The major products of degradation of EP include -OH (3400 cm^{-1}-3700 cm^{-1}), CO_2 (2359 cm^{-1}), C-O and C-H of bisphenol A (1251 cm^{-1},1331 $cm^{-1}$and 1175cm^{-1}), aromatic compounds (3034 cm^{-1}, 1509 cm^{-1},1606cm^{-1} and 831 cm^{-1}), C-H of aliphatic compounds (2850 cm^{-1}-3100 cm^{-1}). Compared with the spectrum of EP, there are no emerging peaks in the spectrum of 20DOPO-BAPh/EP. However, significant changes in peak intensity are observed. For example, the peak of 1250 cm^{-1} (P=O) overlaps with the C-O and C-H characteristic peaks of bisphenol A, leading to an increase in peak height. And the heightened peak at 750cm^{-1} is the contribution of the presence of the DOPO group. This proved that the products with polyphosphate-containing structures were formed during the pyrolysis of DOPO-BAPh. Besides, the compounds containing polyphosphate structure react with other products of decomposition to form P-O-Ph (1606 cm^{-1}) bonds during the decomposition [43].

3.6. Microscopic morphologies of char residues

The char residuals created during the decomposition plays an essential role in limiting heat transfer and flame spread [44]. Therefore, the char residues after cone calorimetry tests were analysed by SEM to evaluate the flame-retardant mechanism of EPs with the addition of DOPO-BAPh. The SEM images of the surface morphology of the residual chars are shown in Fig. 11. It can be observed that the char residuals of EP show large cracks and holes in the surface, which was a channel for heat and fuel transfer. The char residuals became denser with increasing additive content. As shown in Fig. 11(e), the char layers of 20DOPO-BAPh/EP exhibited a continuous surface. Such integrated char layers play a primary role in limiting heat transfer and protecting the internal matrix [8], which contributes to the epoxy thermosets achieving V-0 in UL-94 testing. In addition, several bubbles separated by charcoal layers were observed, indicating the dense char layer prevented the release of pyrolysis gases and thus forming an expanded structure. The primary contribution is due to the self-cured of nitrile groups to form the stable species with network structure. Consequently, the flame retardancy of DOPO-BAPh/EP composites was enhanced.

Fig. 12 shows the chemical components of residual chars after the cone calorimeter tests performed by XPS. Table 5 presents the percentage of atoms for elemental elements in the residual chars. It is noticed that the carbon content in the residual char of DOPO-BAPh/EP increased markedly compared to EP, suggesting that DOPO-BAPh impede the oxidation of the residual chars. The reason is attributed to the formation of network structured species from the nitrile group via self-cured, which protects the

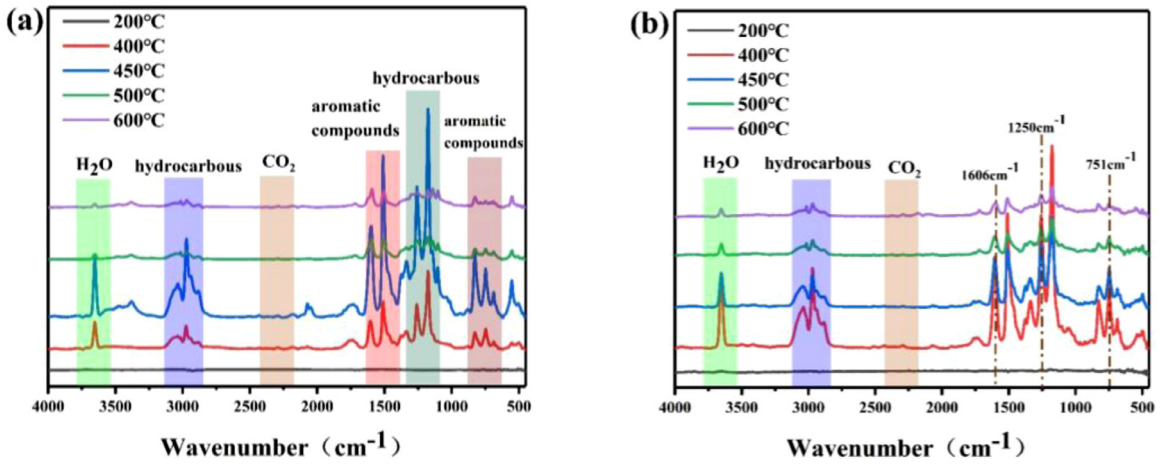

Fig. 10. FTIR spectra of gaseous pyrolysis products of (a) EP and (b) 20DOPO-BAPh/EP at different stages of decomposition.

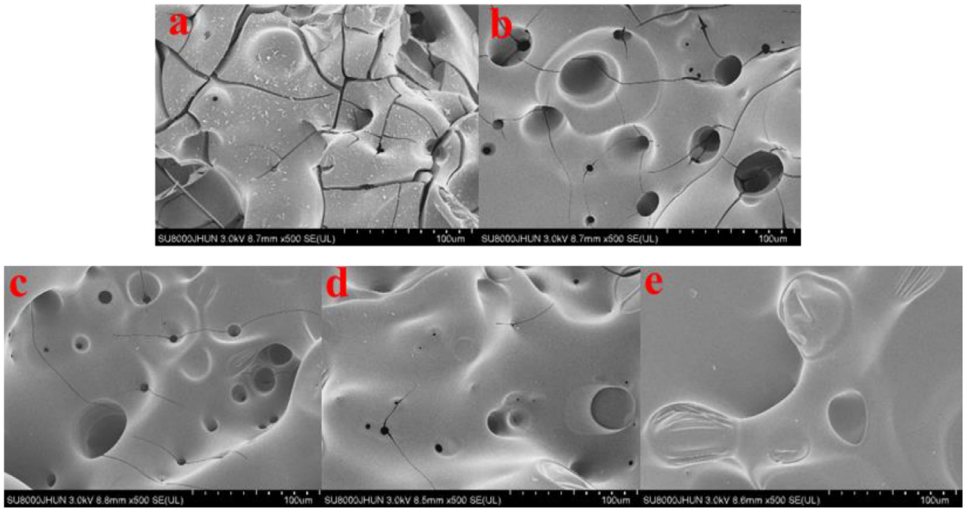

Fig. 11. . SEM images of the surface morphology of char residues: (a) EP, (b) 5DOPO-BAPh/EP, (c) 10DOPO-BAPh/EP, (d) 15DOPO-BAPh/EP, (e) 20DOPO-BAPh/EP.

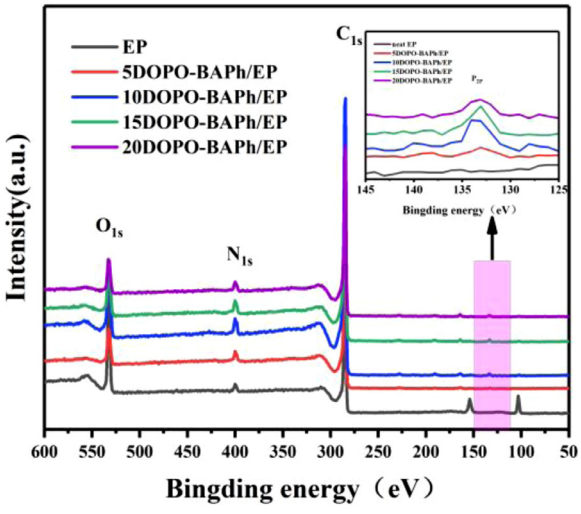

Fig. 12. XPS survey spectra of residual chars after the cone calorimeter tests.

Table 5
The elemental contents of the residual chars evaluated by XPS.

Samples	Element concentration (%)			
	C	O	N	P
EP	70.45	26.61	2.94	0
5DOPO-BAPh/EP	86.3	9.17	4.26	0.27
10DOPO-BAPh/EP	83.57	12.1	3.82	0.51
15DOPO-BAPh/EP	82.45	12.1	4.86	0.59
20DOPO-BAPh/EP	85.86	9.36	4.27	0.52

char layer formed during combustion from thermal radiation. The oxygen content in DOPO-BAPh/EP is found to be significantly decreased than EP. This demonstrated the ability of DOPO-BAPh to facilitate the generation of residual char during combustion. Moreover, the presence of P-elements was detected in the residual char of DOPO-BAPh/EP, demonstrating the contribution of phosphorus elements in both the condensed and gas phases.

Fig. 13 presents the C_{1s}, N_{1s}, O_{1s}, and P_{2p} spectrum of residual chars of 20DOPO-BAPh/EP. The C_{1s} spectra are shown in Fig. 13(a). It can be observed that there are three peaks in spectra. The peak at 284.8 eV was the contribution of C-H and C-C in aliphatic and aromatic compounds. The spectral bands at around 286.1 eV were attributed to the presence of C-O-C, C-O-P, and C-N bonds. Further, the binding energy of 289.2 eV can be corresponding to the carbonyl groups. For the O_{1s} spectra, there are three peaks at around 533.2, 532.2, and 530.8 eV. The peak relative to the double oxygen bonds on carbonyl or phosphate groups located at 530.8 eV.

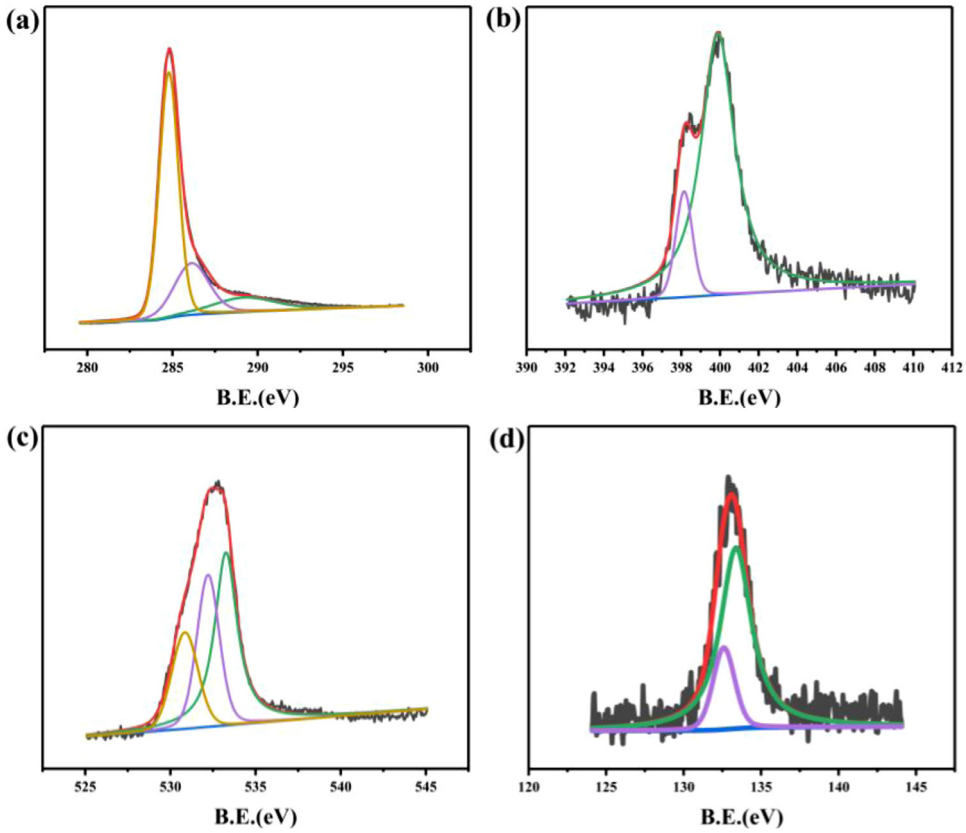

Fig. 13. High resolution of (a) C_{1s}, (b) N_{1s}, (c) O_{1s}, and (d) P_{2p} spectra of residual char of 20DOPO-BAPh/EP.

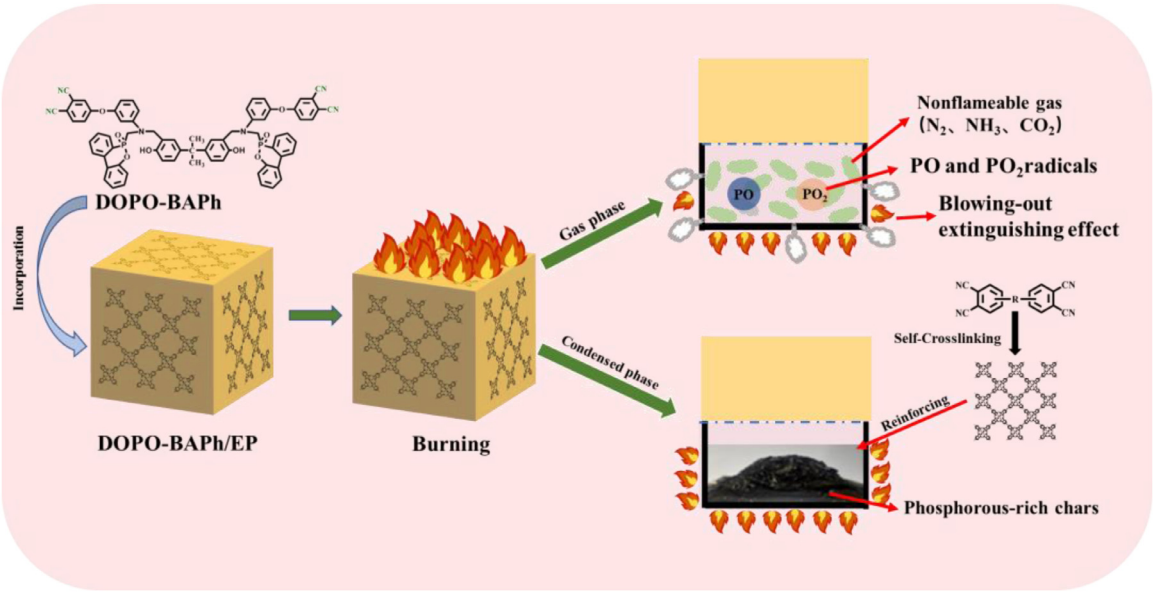

Scheme 2. Flame retardant mechanism of DOPO-BAPh/EP thermosets.

The spectral bands at around 532.2 eV can be attributed to -O- in C-O-C or C-O-P groups. The signal at 533.2 eV can be assigned to C-OH. The spectral peak of N_{1s} can be divided into two components of 399.9 and 398.1 eV, assigning to C-N and C=N, respectively. For the P_{2p} spectra, The P_{2p} peak was separated into two peaks. The signal at 132.5 eV was the contribution of P-O-C or PO_3 groups in phosphate. Another peak in 133.3 eV was attributed to P_2O_5. The results suggested that the DOPO-BAPh/EP thermosets generated phosphate structure-containing products during thermal degradation, which can be dehydrated and esterified to form the protective char layer.

3.7. Mechanism of flame retardancy

Diagram of the flame-retardation mechanism of DOPO-BAPh on EP is shown in Scheme 2. The mechanism is attributed to the quenching effect and the dilution effect on the released free radicals in the gas phase, and the protection of the dense char

layers formed during the combustion in the condensed phase. In the gas phase, DOPO-BAPh-modified epoxy thermosets release phosphorus-containing radicals and non-flammable gases during pyrolysis. On the one hand, phosphorus-containing radicals can extinguish reactive radicals such as H•, O•, and HO• in the flame and suppress the flame intensity [45,46]. On the other hand, non-flammable gases play an important role by diluting combustible gases. In addition, the blowing-out effect during the combustion contributed to the flame-regarding effect. In the condensed phase, as thermal decomposition continues, the polyphosphoric acid compounds formed by modified epoxy thermosets catalyse the dehydration of the degraded EP to form the phosphorus-rich chars. Further, the nitrile group within DOPO-BAPh is able to self-crosslink to form the species with network-structure, reinforcing the stability of the char layer formed during combustion [34]. In summary, the modified epoxy thermosets exhibit flame retardancy in both the gas phase and condensed phase.

4. Conclusion

A phosphorus/nitrogen containing compound was synthesized as a flame retardant for EP by grafting reaction using DOPO and BAPh. A series of epoxy composites containing the DOPO-BAPh additive was prepared using DDS as a curing agent. The results showed that the introduction of DOPO-BAPh accelerated the curing of EPs. Further, the introduction of DOPO-BAPh conferred flame retardancy to EP, resulting in modified epoxy thermosets with low heat release intensity and LOI values, and all samples scored the V-0 rating in UL-94 testing. Epoxy thermosets achieved flame retardancy at low phosphorus-contents. The low loading of DOPO-BAPh loading (only 0.26 wt.% phosphorus content) leads to a marked enhancement in flame retardant properties: the LOI value achieved 35.8% and passed the UL-94 V-0 testing. The flame-retardation mechanism of DOPO-BAPh on EP was examined using TG-IR, SEM, and XPS. The results revealed that DOPO-BAPh primarily contributes to the quenching effect of the released free radicals and the dilution effect of non-flammable gases in the gas phase and the barrier effect of phosphorus-rich chars of the condensed phase. We believe that DOPO-BAPh/EP thermoset could be a potential candidate for high-performance engineering applications in the future.

Declaration of Competing Interest

The authors declare that they have no known competing financial interests or personal relationships that could have appeared to influence the work reported in this paper.

CRediT authorship contribution statement

Donghui Wang: Investigation, Data curation, Writing - original draft. **Quanyi Liu:** Supervision, Funding acquisition. **Xiaoliang Peng:** Methodology, Writing - review & editing. **Chuanbang Liu:** Investigation. **Zekun Li:** Methodology. **Zhifa Li:** Investigation. **Rui Wang:** Investigation. **Penglun Zheng:** Supervision, Formal analysis, Writing - review & editing. **Hui Zhang:** Supervision.

Acknowledgement

The authors are greatly appreciating the funding support of National Key R&D Program of China (No. 2018YFC0809500), the National Natural Science Foundation of China (Grant No. U1633203, U1733126), General Program of Civil Aviation Flight University of China (Grant No. J2020-111) and Sichuan Science and Technology Program (NO. 2018GZYZF0069).

References

[1] FK Özmen, ME Üreyen, AS. Koparal, Cleaner production of flame-retardant–glass reinforced epoxy resin composite for aviation and reducing smoke toxicity, J Clean Prod (2020) 124065.
[2] B Perret, B Schartel, K Stöß, M Ciesielski, J Diederichs, M Döring, et al., Novel DOPO-based flame retardants in high-performance carbon fibre epoxy composites for aviation, Eur Polym J 47 (5) (2011) 1081–1089.
[3] L Greiner, P Kukla, S Eibl, M. Döring, Phosphorus containing polyacrylamides as flame retardants for epoxy-based composites in aviation, Polymers-Basel 11 (2) (2019) 284.
[4] S Huo, S Yang, J Wang, J Cheng, Q Zhang, Y Hu, et al., A liquid phosphorus-containing imidazole derivative as flame-retardant curing agent for epoxy resin with enhanced thermal latency, mechanical, and flame-retardant performances, J Hazard Mater 386 (2020) 121984.
[5] P Wang, Z. Cai, Highly efficient flame-retardant epoxy resin with a novel DOPO-based triazole compound: Thermal stability, flame retardancy and mechanism, Polym Degrad Stabil 137 (2017) 138–150.
[6] X Wang, Y Hu, L Song, W Xing, H. Lu, Preparation, flame retardancy, and thermal degradation of epoxy thermosets modified with phosphorous/nitrogen-containing glycidyl derivative, Polym Advan Technol 23 (2) (2012) 190–197.
[7] L Qian, L Ye, Y Qiu, S. Qu, Thermal degradation behavior of the compound containing phosphaphenanthrene and phosphazene groups and its flame retardant mechanism on epoxy resin, Polymer 52 (24) (2011) 5486–5493.
[8] L Qian, Y Qiu, N Sun, M Xu, G Xu, F Xin, et al., Pyrolysis route of a novel flame retardant constructed by phosphaphenanthrene and triazine-trione groups and its flame-retardant effect on epoxy resin, Polym Degrad Stabil 107 (2014) 98–105.
[9] DM Patil, GA Phalak, ST. Mhaske, Novel phosphorus-containing epoxy resin from renewable resource for flame-retardant coating applications, J Coat Technol Res 16 (2) (2019) 531–542.
[10] T-P Ye, S-F Liao, Y Zhang, M-J Chen, Y Xiao, X-Y Liu, et al., Cu (0) and Cu (II) decorated graphene hybrid on improving fireproof efficiency of intumescent flame-retardant epoxy resins, Compos Part B-Eng 175 (2019) 107189.
[11] L-P Gao, D-Y Wang, Y-Z Wang, J-S Wang, B Yang, A flame-retardant epoxy resin based on a reactive phosphorus-containing monomer of DODPP and its thermal and flame-retardant properties, Polym Degrad Stabil 93 (7) (2008) 1308–1315.
[12] S Yang, Y Hu, Q. Zhang, Synthesis of a phosphorus–nitrogen-containing flame retardant and its application in epoxy resin, High Perform Polym 31 (2) (2019) 186–196.
[13] S Yang, J Wang, S Huo, L Cheng, M. Wang, Preparation and flame retardancy of an intumescent flame-retardant epoxy resin system constructed by multiple flame-retardant compositions containing phosphorus and nitrogen heterocycle, Polym Degrad Stabil 119 (2015) 251–259.
[14] J-L Li, C Wang, K-Y. Lu, Enhanced cryogenic mechanical properties and liquid oxygen compatibility of DOPO-containing epoxy resin reinforced by epoxy–grafted polysiloxane, Polym Bull 77 (7) (2020) 3429–3442.
[15] B Liu, C Jiang, C Zhang, X Bai, J. Mu, Octasilsesquioxane-reinforced TMBP epoxy nanocomposites: Characterization of thermal, flame-retardant, and morphological properties, High Perform Polym 24 (8) (2012) 747–755.
[16] W Yan, J Yu, M Zhang, S Qin, T Wang, W Huang, et al., Flame-retardant effect of a phenethyl-bridged DOPO derivative and layered double hydroxides for epoxy resin, Rsc Adv 7 (73) (2017) 46236–46245.
[17] S Liu, Z Fang, H Yan, H. Wang, Superior flame retardancy of epoxy resin by the combined addition of graphene nanosheets and DOPO, Rsc Adv 6 (7) (2016) 5288–5295.
[18] S Qiu, X Wang, B Yu, X Feng, X Mu, RK Yuen, et al., Flame-retardant-wrapped polyphosphazene nanotubes: A novel strategy for enhancing the flame retardancy and smoke toxicity suppression of epoxy resins, J Hazard Mater 325 (2017) 327–339.
[19] R Chen, K Hu, H Tang, J Wang, F Zhu, H. Zhou, A novel flame retardant derived from DOPO and piperazine and its application in epoxy resin: flame retardance, thermal stability and pyrolysis behavior, Polym Degrad Stabil 166 (2019) 334–343.
[20] X Wang, Y Hu, L Song, W Xing, H Lu, P Lv, et al., Flame retardancy and thermal degradation mechanism of epoxy resin composites based on a DOPO substituted organophosphorus oligomer, Polymer 51 (11) (2010) 2435–2445.
[21] Y Feng, C He, Y Wen, Y Ye, X Zhou, X Xie, et al., Improving thermal and flame retardant properties of epoxy resin by functionalized graphene containing phosphorous, nitrogen and silicon elements, Compos Part A-Appl S 103 (2017) 74–83.
[22] B Oktay, E. Çakmakçi, DOPO tethered Diels Alder clickable reactive silica nanoparticles for bismaleimide containing flame retardant thiol-ene nanocomposite coatings, Polymer 131 (2017) 132–142.
[23] S Liu, J Chen, J Zhao, Z Jiang, Y. Yuan, Phosphaphenanthrene-containing borate ester as a latent hardener and flame retardant for epoxy resin, Polym Int 64 (9) (2015) 1182–1190.
[24] P Wang, L Chen, H Xiao, T. Zhan, Nitrogen/sulfur-containing DOPO based oligomer for highly efficient flame-retardant epoxy resin, Polym Degrad Stabil 171 (2020) 109023.
[25] Z-M Zhu, L-X Wang, X-B Lin, L-P. Dong, Synthesis of a novel phosphorus-nitrogen flame retardant and its application in epoxy resin, Polym Degrad Stabil 169 (2019) 108981.

[26] H Luo, W Rao, P Zhao, L Wang, Y Liu, C. Yu, An efficient organic/inorganic phosphorus–nitrogen–silicon flame retardant towards low-flammability epoxy resin, Polym Degrad Stabil (2020) 109195.
[27] S Tang, L Qian, Y Qiu, Y. Dong, High-performance flame retardant epoxy resin based on a bi-group molecule containing phosphaphenanthrene and borate groups, Polym Degrad Stabil 153 (2018) 210–219.
[28] M Xu, D Ren, L Chen, K Li, X. Liu, Understanding of the polymerization mechanism of the phthalonitrile-based resins containing benzoxazine and their thermal stability, Polymer 143 (2018) 28–39.
[29] M Xu, K Jia, X. Liu, Effect of bisphenol-A on the structures and properties of phthalonitrile-based resin containing benzoxazine, Express Polymer Letters 9 (6) (2015).
[30] S Sun, Y He, X Wang, D. Wu, Flammability characteristics and performance of halogen-free flame-retarded polyoxymethylene based on phosphorus–nitrogen synergistic effects, J Appl Polym Sci 118 (1) (2010) 611–622.
[31] Y Yan, B. Liang, Flame-retardant behavior and mechanism of a DOPO-based phosphorus–nitrogen flame retardant in epoxy resin, High Perform Polym 31 (8) (2019) 885–892.
[32] Y Zhang, B Yu, B Wang, KM Liew, L Song, C Wang, et al., Highly effective P–P synergy of a novel DOPO-based flame retardant for epoxy resin, Ind Eng Chem Res 56 (5) (2017) 1245–1255.
[33] H Guo, Y Zou, Z Chen, J Zhang, Y Zhan, J Yang, et al., Effects of self-promoted curing behaviors on properties of phthalonitrile/epoxy copolymer, High Perform Polym 24 (7) (2012) 571–579.
[34] M Xu, X Yang, R Zhao, X. Liu, Copolymerizing behavior and processability of benzoxazine/epoxy systems and their applications for glass fiber composite laminates, J Appl Polym Sci 128 (2) (2013) 1176–1184.
[35] M-J Xu, G-R Xu, Y Leng, B. Li, Synthesis of a novel flame retardant based on cyclotriphosphazene and DOPO groups and its application in epoxy resins, Polym Degrad Stabil 123 (2016) 105–114.
[36] B Francis, S Thomas, J Jose, R Ramaswamy, VL. Rao, Hydroxyl terminated poly (ether ether ketone) with pendent methyl group toughened epoxy resin: miscibility, morphology and mechanical properties, Polymer 46 (26) (2005) 12372–12385.
[37] W Zhang, X Li, R. Yang, Pyrolysis and fire behaviour of epoxy resin composites based on a phosphorus-containing polyhedral oligomeric silsesquioxane (DOPO-POSS), Polym Degrad Stabil 96 (10) (2011) 1821–1832.
[38] L Li, X Liu, X Shao, L Jiang, K Huang, S. Zhao, Synergistic effects of a highly effective intumescent flame retardant based on tannic acid functionalized graphene on the flame retardancy and smoke suppression properties of natural rubber, Compos Part A-Appl S 129 (2020) 105715.
[39] Y Bai, X Wang, D. Wu, Novel cyclolinear cyclotriphosphazene-linked epoxy resin for halogen-free fire resistance: synthesis, characterization, and flammability characteristics, Ind Eng Chem Res 51 (46) (2012) 15064–15074.
[40] S Jin, L Qian, Y Qiu, Y Chen, F. Xin, High-efficiency flame retardant behavior of bi-DOPO compound with hydroxyl group on epoxy resin, Polym Degrad Stabil 166 (2019) 344–352.
[41] K Zeng, H Hong, S Zhou, D Wu, P Miao, Z Huang, et al., A new soluble aramide with pendant phthalonitrile units and polymer property enhancement by nitrile cure reactions, Polymer 50 (21) (2009) 5002–5006.
[42] M Sumner, M Sankarapandian, J McGrath, J Riffle, U. Sorathia, Flame retardant novolac–bisphthalonitrile structural thermosets, Polymer 43 (19) (2002) 5069–5076.
[43] L Long, J Yin, W He, S Qin, J. Yu, Influence of a phenethyl-bridged DOPO derivative on the flame retardancy, thermal properties, and mechanical properties of poly (lactic acid), Ind Eng Chem Res 55 (40) (2016) 10803–10812.
[44] EN Kalali, X Wang, D-Y. Wang, Multifunctional intercalation in layered double hydroxide: toward multifunctional nanohybrids for epoxy resin, J Mater Chem A 4 (6) (2016) 2147–2157.
[45] GH Hsiue, SJ Shiao, HF Wei, WJ Kuo, YA. Sha, Novel phosphorus-containing dicyclopentadiene-modified phenolic resins for flame-retardancy applications, J Appl Polym Sci 79 (2) (2001) 342–349.
[46] A Schäfer, S Seibold, W Lohstroh, O Walter, M. Döring, Synthesis and properties of flame-retardant epoxy resins based on DOPO and one of its analog DPPO, J Appl Polym Sci 105 (2) (2007) 685–696.